Johanna Guzman,[1,2] Alexandra N. Jauregui,[1] Sandra Merscher-Gomez,[2] Dony Maiguel,[1] Cristina Muresan,[2] Alla Mitrofanova,[2] Ana Diez-Sampedro,[3] Joel Szust,[1] Tae-Hyun Yoo,[2,4] Rodrigo Villarreal,[1,2] Christopher Pedigo,[2] R. Damaris Molano,[1] Kevin Johnson,[1] Barbara Kahn,[5] Bjoern Hartleben,[6] Tobias B. Huber,[6] Jharna Saha,[7] George W. Burke III,[4] E. Dale Abel,[8] Frank C. Brosius,[7] and Alessia Fornoni[1,2]

Podocyte-Specific GLUT4-Deficient Mice Have Fewer and Larger Podocytes and Are Protected From Diabetic Nephropathy

Podocytes are a major component of the glomerular filtration barrier, and their ability to sense insulin is essential to prevent proteinuria. Here we identify the insulin downstream effector GLUT4 as a key modulator of podocyte function in diabetic nephropathy (DN). Mice with a podocyte-specific deletion of GLUT4 (G4 KO) did not develop albuminuria despite having larger and fewer podocytes than wild-type (WT) mice. Glomeruli from G4 KO mice were protected from diabetes-induced hypertrophy, mesangial expansion, and albuminuria and failed to activate the mammalian target of rapamycin (mTOR) pathway. In order to investigate whether the protection observed in G4 KO mice was due to the failure to activate mTOR, we used three independent in vivo experiments. G4 KO mice did not develop lipopolysaccharide-induced albuminuria, which requires mTOR activation. On the contrary, G4 KO mice as well as WT mice treated with the mTOR inhibitor rapamycin developed worse adriamycin-induced nephropathy than WT mice, consistent with the fact that adriamycin toxicity is augmented by mTOR inhibition. In summary, GLUT4 deficiency in podocytes affects podocyte nutrient sensing, results in fewer and larger cells, and protects mice from the development of DN. This is the first evidence that podocyte hypertrophy concomitant with podocytopenia may be associated with protection from proteinuria.

Diabetes 2014;63:701–714 | DOI: 10.2337/db13-0752

Ever since it was demonstrated that insulin infusion can induce an acute transient increase in albumin excretion rate (1), the possibility of a direct effect of insulin signaling in glomerular cell function has been suggested. In fact, insulin resistance correlates with the development of microalbuminuria in patients with either type 1 or type 2 diabetes (2–5), in their siblings (6,7), and in subjects without diabetes (8). Furthermore, impaired insulin sensitivity in diabetic patients is associated with altered renal cell glucose metabolism that may directly

[1]Diabetes Research Institute, Miller School of Medicine, University of Miami, Miami, FL
[2]Department of Medicine, Division of Nephrology and Hypertension, Miller School of Medicine, University of Miami, Miami, FL
[3]Department of Physiology, Miller School of Medicine, University of Miami, Miami, FL
[4]Department of Surgery, Miller School of Medicine, University of Miami, Miami, FL
[5]Department of Medicine, Beth Israel Deaconess Medical Center, Harvard Medical School, Boston, MA
[6]Division of Nephrology, Freiburg University, Freiburg, Germany
[7]Division of Nephrology, University of Michigan, Ann Arbor, MI
[8]Division of Endocrinology, Metabolism and Diabetes and Program in Molecular Medicine, University of Utah, Salt Lake City, UT

Corresponding author: Alessia Fornoni, afornoni@med.miami.edu.

Received 8 May 2013 and accepted 2 October 2013.

This article contains Supplementary Data online at http://diabetes.diabetesjournals.org/lookup/suppl/doi:10.2337/db13-0752/-/DC1.

contribute to progressive renal damage independently of hyperglycemia (5). The evidence that a renal disease resembling diabetic nephropathy (DN) (9) may develop in some of the patients with genetic mutations in the insulin receptor (IR) supports an important role for functional insulin signaling in individuals with renal disease and provides the rationale for interventions that target different elements of the IR signaling cascade.

Podocytes are glomerular cells of the kidney that depend on the integrity of their actin cytoskeleton to prevent the development of microalbuminuria (10). Podocytes have been reported to be a target of insulin (11) and to become insulin resistant prior to the development of microalbuminuria in animal models of diabetes (12). Mice with a podocyte-specific deletion of the IR gene develop a phenotype resembling DN in the absence of hyperglycemia (13,14), suggesting that insulin signaling regulates podocyte function independently of blood glucose levels. Traditionally, the final step in insulin action is physiological modulation of glucose uptake and metabolism (15). Thus, disrupting glucose uptake by facilitative GLUTs might negatively affect podocytes in a manner similar to that observed in IR-deficient podocytes. However, glucose uptake and metabolism may also affect nutrient-sensing pathways independently of insulin signaling (16). In particular, the AMP-activated protein kinase (AMPK) (17) and the mammalian target of rapamycin (mTOR) pathways (18,19) are key direct modulators of podocyte function that can be affected by intracellular glucose.

Podocytes express several GLUTs (1–4,8) that are modulated by high glucose levels and by diabetes (11, 20–22). The overexpression of GLUT1 in mesangial cells leads to a phenotype resembling DN (23) and is associated with an upregulation of mTOR (24). This is not the case for podocytes, where podocyte-specific overexpression of GLUT1 prevents mesangial expansion (25), suggesting the presence of cell-type–specific functions of GLUTs. In this study, we hypothesized that podocyte GLUT4 deficiency mitigates mTOR-dependent signaling independently of insulin signaling, thus protecting mice not only from the development of DN but also from other experimental models of proteinuria associated with mTOR signaling.

RESEARCH DESIGN AND METHODS

Patient Cohort

Kidney samples and results of serology and urinalysis of the patients were made available through the organ procurement agency of our institution, and the Institutional Review Board at the University of Miami (Miami, FL) approved their use. Briefly, kidney biopsy samples were collected by the organ procurement agency from three patients with type 1 diabetes, normoalbuminuria, and high glomerular filtration rate; from six patients with type 1 diabetes and microalbuminuria; and from six age- and sex-matched patients without diabetes. In addition, three patients with hypertensive nephrosclerosis were studied.

Mice Utilization and Killing

Twenty B6.Cg-m$^{+/+}$ Lepr^{db}/Lepr^{db} (*db*/*db*) and 16 B6.Cg-m$^{+/+}$ Lepr$^{db/+}$ (*db*/+) female mice were purchased from The Jackson Laboratory (Bar Harbor, ME). All animal procedures were conducted under protocols approved by the Institutional Animal Care and Use Committee. Podocyte-specific GLUT4 KO mice (G4 KO) were generated by breeding floxed GLUT4 mice (26) with podocin-CRE mice (27). Wild-type (WT) and heterozygous (G4 Het) littermates were used as controls. Metabolic measurements were performed weekly until mice sacrifice. Systolic blood pressure was measured at 32 weeks using a noninvasive tail cuff blood pressure unit and BpMonWin software (IITTC Life Science, Inc., Woodland Hills, CA) as previously reported (28). At the time they were killed, mice were perfused with isotonic saline, and tissue was collected for histological analysis and glomeruli isolation.

Experimental Models of Proteinuria

For lipopolysaccharide (LPS) injection, we used an intraperitoneal injection of 300 μg ultrapure LPS (Sigma) in mice that was shown in prior studies to induce proteinuria (29). Spot morning urine samples of all mice at time points 0, 12, 24, 36, 48, 60, and 72 h were collected, and mice were killed at 72 h, as described above. In a second experiment aimed at the collection of glomerular lysates and tissue sections after LPS injection, six mice per group were studied, and tissue and glomerular lysate samples were collected at 36 h, prior to the recovery from proteinuria. For the induction of diabetes, we performed intraperitoneal injections of streptozotocin (50 mg/kg daily on 5 consecutive days). For adriamycin experiments, 12-week–old mice were challenged with a single injection of adriamycin (20 mg/kg). Four G4 KO and four WT mice on a mixed background were exposed to adriamycin. Three mice per group served as controls. Urine was collected every other day for the first week and then weekly for 4 weeks. Mice were killed as described above. For rapamycin experiments, adriamycin-treated G4 KO and WT mice were concomitantly injected with rapamycin (1 mg/kg/day i.p.; InvivoGen), three times per week for 5 weeks. Fasting glucose levels were measured weekly from tail blood samples using a glucometer (Bayer, Pittsburgh, PA). Albumin content was measured weekly by ELISA (Bethyl Laboratories, Montgomery, TX). Urinary creatinine was assessed by an assay based on the Jaffe method (Stanbio, San Antonio, TX). Values are expressed as micrograms of albumin per milligram of creatinine.

Assessment of Mesangial Expansion, Glomerular Surface Area, and Podocyte Number and Size

Periodic acid Schiff (PAS) staining of 4-μm-thick slides was performed for the quantitative analysis of mesangial

expansion calculated as the percentage of the total glomerular area that was PAS-positive, as previously reported (30). For podocyte counts, paraffin-embedded, paraformaldehyde-fixed tissue was sectioned at 3 and 9 μm, as previously published (30). Glomerular volume per podocyte (GV/P) is a variable that incorporates the relationship between both podocyte number and glomerular basement membrane surface area, is the reciprocal of podocyte density, and is a useful measure of the degree of podocyte reserve (31). Measurements of the GLEPP1-positive area were performed in 50 consecutive glomerular tuft areas, and the individual podocyte volume was determined by dividing the mean GLEPP1-positive (podocyte) volume per glomerulus by the mean podocyte number, as previously described (32).

Immunofluorescence Staining

A standard immunofluorescence protocol was followed using the following primary antibodies: polyclonal guinea pig anti-nephrin antibody from Fitzgerald (Acton, MA); rabbit polyclonal anti-GLUT4 antibody (EMD Millipore, Billerica, MA); rabbit polyclonal anti-GLUT1 antibody (EMD Millipore); rabbit polyclonal anti-synaptopodin antibody (gift of Dr. Peter Mundel); mouse monoclonal anti-active Ras homolog gene family member A (RhoA) antibody (New East Biosciences, Malvern, PA); and rabbit polyclonal anti-pS6 antibody (4858s; Cell Signaling Technology). Alexa Fluor-conjugated secondary antibodies from Invitrogen were used, and images were acquired by confocal microscopy and quantified using ImageJ.

Podocyte Culture, Western Blotting, and Cell Size Analysis

Primary podocytes were isolated as previously described (12). Protein concentrations of each sample prepared with CHAPS buffer were measured using the DC protein assay (Bio-Rad, Carlsbad, CA), and an equal amount of protein was loaded onto 4–20% SDS-PAGE gels (Bio-Rad) and transferred to nitrocellulose membranes (Bio-Rad) for Western blot analysis. The following primary antibodies were used: mouse monoclonal anti-Glut4 and anti-RhoA and goat polyclonal anti-NPR-B (C-19) (Santa Cruz Biotechnology, Santa Cruz, CA); rabbit anti-Glut1 (EMD Millipore); mouse monoclonal anti-glyceraldehyde-3-phosphate dehydrogenase (GAPDH; Calbiochem); rabbit polyclonal anti-synaptopodin and podocin (gifts of Dr. Peter Mundel); guinea pig anti-nephrin (Fitzgerald); rabbit polyclonal anti-zonula occludens-1 (ZO-1; Zymed); and rabbit polyclonal antiphosphorylated and total S6, P70S6K, AMPK, AKT, mitogen-activated protein kinase (MAPK) 42/44, IKKα, and myeloid differentiation factor-88 (MyD88) (Cell Signaling Technology). Fixed and washed podocyte cell lines were imaged using Opera LX High Content Screening System (PerkinElmer, Waltham, MA) with 10× air-objective or 20× water-objective. Cell area and cell number were determined using Acapella Software (PerkinElmer). For the quantitative measurement of DNA, cells were lysed in T-PER reagent (Pierce, Rockford, IL), and DNA measurement was performed using a Pico-Green Kit (Invitrogen). Annexin V (Vybrant Apoptosis Assay; Invitrogen) staining was used to study apoptosis, and quantitative assessment performed by flow cytometry with BD Diva 6.0 Software (BD LSRII System; BD Biosciences, San Jose, CA). Staurosporine (1 mmol/L for 2 h; Sigma) was used as a positive control.

Small Interfering RNA Experiments

Mouse podocytes were cultured as described. At day 10, cells were exposed to a pool of on-target plus small interfering RNA (siRNA) for GLUT4, GLUT1, AMPKα, and TSC1 (Dharmacon, Lafayette, CO), and on-target plus nontargeting siRNA. After 6, 12, 24, and 48 h, cells were collected in lysis buffer in the presence of protease inhibitors (Bio-Rad) for protein analysis and in sample buffer for the analysis of apoptosis, and were fixed and stained with phalloidin to study the morphology of the actin cytoskeleton. Images were acquired by confocal microscopy as well as by light microscopy. Annexin V (Vybrant Apoptosis Assay; Invitrogen) staining was used to study apoptosis and quantitative assessment performed by flow cytometry with BD Diva 6.0 Software (BD LSRII System; BD Biosciences, San Jose, CA). Staurosporine (1 mmol/L for 2 h; Sigma) was used as a positive control.

Statistical Analysis

All data are shown as means and SDs. Four to eight independent experiments were performed for in vitro studies. Four to fourteen mice per group were used for in vivo experiments, which were repeated twice to allow for statistical analysis of Western blots from glomerular lysates. Statistical analysis was performed with one-way ANOVA. When one-way ANOVA showed statistical significance, results were compared using the *t* test after Tukey correction for multiple comparisons. Results were considered statistically significant at $P < 0.05$.

RESULTS

Glomerular GLUT4 and GLUT1 Expression Are Differentially Modulated at Different Stages of Human and Experimental DN

In normal human glomeruli, GLUT4 colocalizes with synaptopodin-positive podocytes, whereas only partial colocalization of GLUT1 with synaptopodin was detected (Fig. 1*A*). GLUT4 and GLUT1 mRNA expression was studied in microdissected glomeruli from cadaveric patients. Six type 1 diabetic deceased donors with microalbuminuria and normal creatinine and three type 1 diabetic deceased donors with normoalbuminuria and serum creatinine levels <0.6 mg/dL were compared with six age-matched, cold ischemia time- and sex-matched nondiabetic deceased donors with normoalbuminuria and normal creatinine levels (controls) (Supplementary Table 1). GLUT4 expression was significantly upregulated in glomeruli from patients with normoalbuminuria and

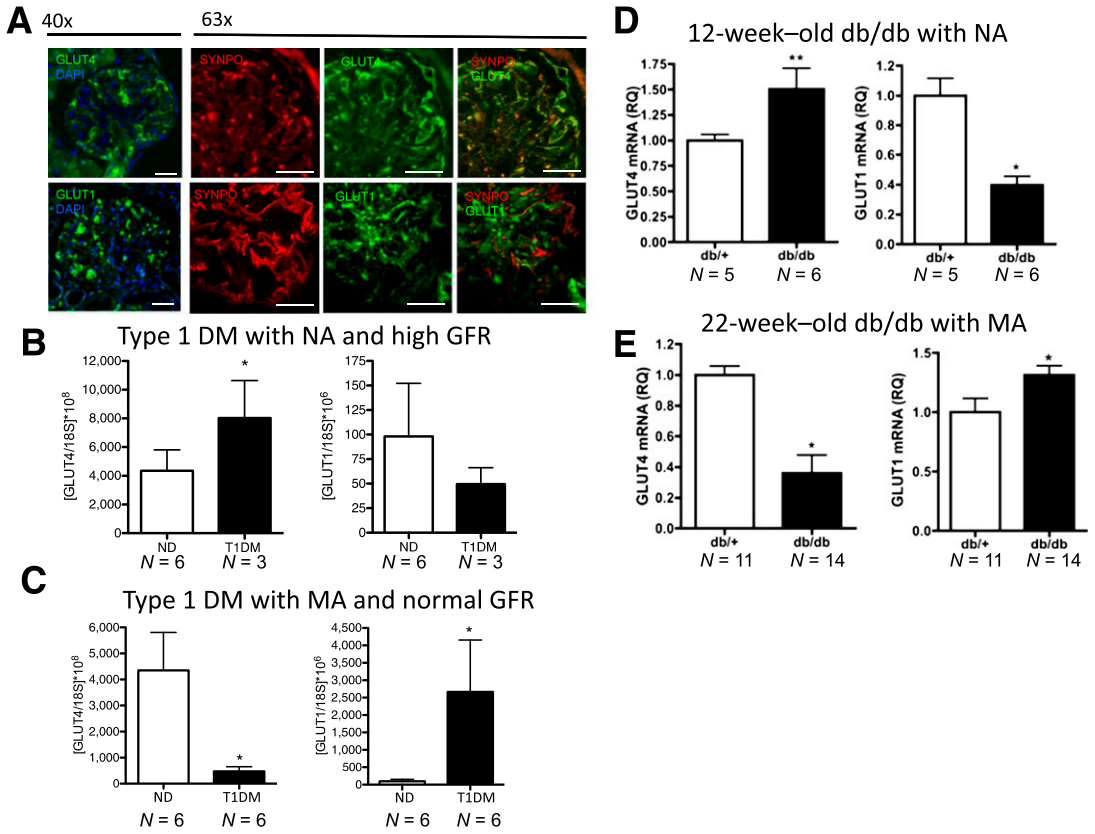

Figure 1—GLUT4 and GLUT1 expression in clinical and experimental DN. *A*: Confocal images of GLUT4 and GLUT1 expression in normal human glomeruli, showing the colocalization with synaptopodin (SYNPO) used as a podocyte-specific marker in the micrographs at higher magnification. Scale bar: 25 μm. *B*: Glomerular GLUT4 mRNA expression is upregulated in patients with type 1 diabetes mellitus (type 1 DM and T1DM), normoalbuminuria, and low serum creatinine levels. *C*: Once microalbuminuria is established, GLUT4 mRNA is downregulated when compared with nondiabetic controls (ND). The opposite is true for GLUT1. *D* and *E*: Bar graph analysis of GLUT4 and GLUT1 expression in glomeruli isolated from *db*/*db* and *db*/+ mice at 12 and 22 weeks of age. The number of mice used for each experiment is also shown. $^{**}P < 0.001$, $^{*}P < 0.05$. NA, normoalbuminuria; MA, microalbuminuria; GFR, glomerular filtration rate.

serum creatinine <0.6 mg/dL with very low creatinine levels when compared with controls (Fig. 1*B*). Glomeruli from patients with microalbuminuria and normal creatinine levels were characterized by decreased GLUT4 expression ($P < 0.05$) and increased GLUT1 expression ($P < 0.05$) when compared with nondiabetic patients (Fig. 1*C*) and to three patients with hypertensive glomerulosclerosis (data not shown). A similar pattern of GLUT4 and GLUT1 expression was observed in normoalbuminuric 12-week–old *db*/*db* mice (Fig. 1*D*) and microalbuminuric 22-week–old *db*/*db* mice when compared with age-matched *db*/+ (12) (Fig. 1*E*). In order to understand whether the increased GLUT4 expression in early nephropathy was of podocyte origin, we used a primary culture of podocytes from *db*/*db* and *db*/+ mice of 12 weeks of age (12), and demonstrated that *db*/*db* podocytes are characterized by increased GLUT4 mRNA and protein expression (Fig. 2*A*), unchanged GLUT1 expression, and increased baseline glucose uptake (Fig. 2*C*), but decreased ability of insulin to cause glucose uptake and GLUT4 translocation to the plasma membrane (Fig. 2*D* and *E*).

Mice With a Podocyte-Specific Deletion of GLUT4 Have No Apparent Renal Phenotype at Baseline

In order to determine whether GLUT4 deficiency has a causative role in DN, we studied podocyte-specific G4 KO mice. While we were able to demonstrate effective recombination by both immunofluorescence and Western blotting (Figs. 3*A* and 4*A*), G4 KO mice did not develop any albuminuria (Fig. 3*B*) or hypertension (Fig. 3*C*) when compared with WT mice. Histological analysis of G4 KO kidney sections revealed unchanged mesangial expansion and glomerular surface area (Fig. 3*D*–*F*). Western blot analysis of isolated glomeruli demonstrated that GLUT4 deficiency was not accompanied by a compensatory increase in GLUT1 (Fig. 4*A*). Furthermore, glomeruli from G4 KO mice were characterized by increased nephrin and podocin expression while ZO-1 and synaptopodin were not modified (Fig. 4*A*). Interestingly, glomeruli from G4 KO mice demonstrated almost undetectable S6 and p70S6 phosphorylation with unchanged AKT and increased AMPK and MAPK42/44 phosphorylation (Fig. 4*B*), suggesting that the ability to suppress AMPK and to

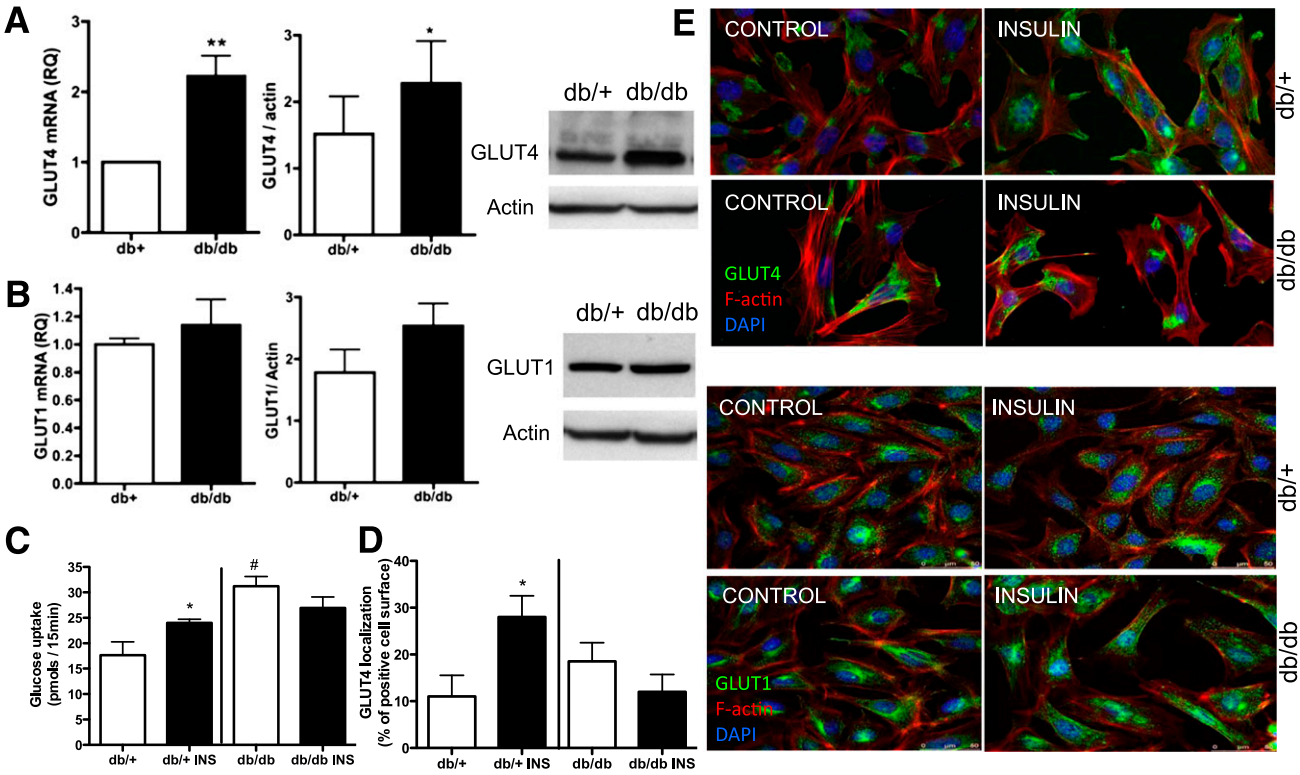

Figure 2—GLUT4 is upregulated in podocytes from *db/db* mice prior to the onset of microalbuminuria. Bar graph is a representation of GLUT4 (*A*) and GLUT1 (*B*) mRNA and protein expression in primary podocytes isolated from *db/db* and *db/+* mice at 12 weeks of age. Four independent experiments were performed, and a representative Western blot is shown. **P* < 0.05, ***P* < 0.01. *C*: Bar graph analysis of three independent glucose uptake experiments performed in *db/+* and *db/db* podocytes in the presence or absence of 100 nmol/L insulin (INS) for 15 min. **P* < 0.05 when comparing insulin to no insulin. #*P* < 0.05 when comparing *db/db* to *db/+* mice. *D*: Bar graph analysis of three independent experiments for the quantification of the percentage of cell membrane from *db/db* and *db/+* podocyte-positive mice for GLUT4 before and after insulin treatment (INS). **P* < 0.05. *E*: Representative GLUT4 and GLUT1 immunofluorescence staining in *db/+* and *db/db* podocytes at baseline and after insulin stimulation. Rhodamine phalloidin is used to stain actin fibers and DAPI is used to stain nuclei. RQ, relative quantification.

activate mTOR is impaired in podocytes of G4 KO mice, while insulin signaling through AKT is preserved.

G4 KO Mice Are Characterized by Decreased Podocyte Number and Increased Podocyte Size

Although G4 KO mice were characterized by a generally normal renal phenotype at baseline, the number of podocytes per glomerulus was significantly lower in G4 KO mice when compared with WT mice (Fig. 5*A*). This phenotype was already apparent at 4 weeks of age. This was accompanied by an equal glomerular volume (Fig. 5*B*), an increased GV/P (Fig. 5*C*), as well as an increase in the GLEPP1-positive area (Fig. 5*D*). Primary podocyte cultures from three different G4 KO mice and three WT mice demonstrated increased podocin, ZO-1, and nephrin expression with unchanged synaptopodin expression (Fig. 5*E*), similar to what we had found on isolated glomeruli (Fig. 5*A*). GLUT4 expression was totally suppressed in primary podocyte cultures from G4 KO mice but was easily detected in cultures from WT mice, further confirming that effective recombination had occurred (Fig. 5*E*). G4 KO cell lines were characterized by increased protein/DNA content (Fig. 5*E*) and increased cell size (Fig. 5*F*) when compared with WT cells. This was not accompanied by increased apoptosis (Fig. 5*G*). The increased cell size was specifically associated with GLUT4 deficiency, as siRNA for GLUT4 in mouse podocytes resulted in increased cell size that was not observed in G1 siRNA–treated podocytes (Fig. 6*A* and *B*). Increased cell size in G4 siRNA–treated podocytes occurred in association with decreased P70S6K phosphorylation and increased AMPK phosphorylation (Fig. 6*C*–*E*), but did not require AMPK or TSC1 expression (Fig. 6*F* and *G*).

Diabetic Mice With a Podocyte-Specific Deletion of GLUT4 Are Protected From Glomerular Hypertrophy and Albuminuria

As enhanced mTOR activity can induce glomerular hypertrophy in diabetes (18,19,33), we tested whether G4 KO mice were protected from hyperglycemia-induced glomerular hypertrophy and albuminuria. Indeed, G4 KO mice were partially protected from the development of glomerular hypertrophy (Fig. 7*A* and *B*). As glomerular hypertrophy in diabetes is a RhoA-dependent phenomenon (34,35), and RhoA activation is linked to mTOR (36), we tested whether glomeruli from G4 KO mice were

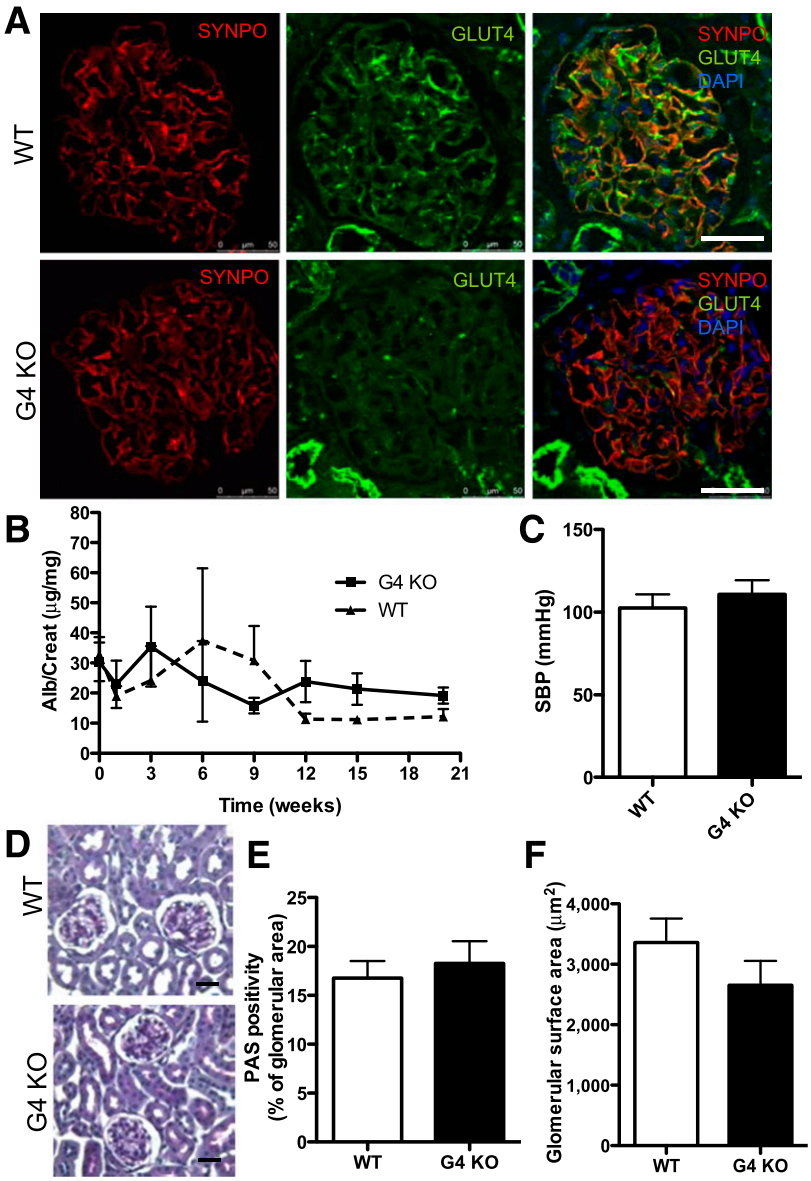

Figure 3—Podocyte-specific G4 KO mice do not have an apparent renal phenotype. *A*: Representative confocal images demonstrating effective deletion of GLUT4 (green) in podocytes identified as synaptopodin (SYNPO)-positive cells (red). *B*: Time course analysis of urinary albumin/creatinine (Alb/Creat) ratios in morning urine collection in G4 KO and WT mice (n = 6 each). *C*: Bar graph analysis of systolic blood pressure (SBP) measurements at 32 weeks demonstrating no difference between WT and G4 KO mice. *D*: Representative PAS staining of renal cortex of WT and G4 KO mice. Scale bar: 25 μm. *E*: Bar graph analysis of mesangial expansion in G4 KO and WT mice (n = 6 each). *F*: Quantitative evaluation of glomerular surface area in WT and G4 KO mice (in square micrometers). DAPI, 4′,6-diamidino-2-phenylindole.

characterized by a decreased RhoA activity and/or expression. Active RhoA was increased in diabetic WT mice when compared with WT controls but was not modified by diabetes in G4 KO mice (Fig. 7*C*). In addition, while diabetes increased total RhoA levels in WT glomeruli, G4 KO glomeruli showed decreased RhoA levels at baseline, and RhoA did not increase after the induction of diabetes (Fig. 7*D*). G4 KO mice were partially protected from the development of albuminuria at 12 weeks (Fig. 7*E*), and this trend was preserved at 24 weeks (Fig. 7*F*) and at 32 weeks (Fig. 7*G*). At 32 weeks, quantitative evaluation of PAS-positive material demonstrated a significant reduction of PAS-positive glomerular area in G4 KO diabetic mice when compared with diabetic WT mice (Fig. 7*H* and *I*). Diabetes caused a further significant reduction in podocyte number in both WT and G4 KO mice (Fig. 7*J*). Unlike WT mice, glomeruli from G4 KO mice were protected from increased S6 phosphorylation in response to hyperglycemia (Fig. 7*K*). Blood glucose level, body weight, and kidney weight were not different among WT, G4 Het, and G4 KO diabetic mice: mean body weights at the time the mice were killed were 25, 24, and 26 g,

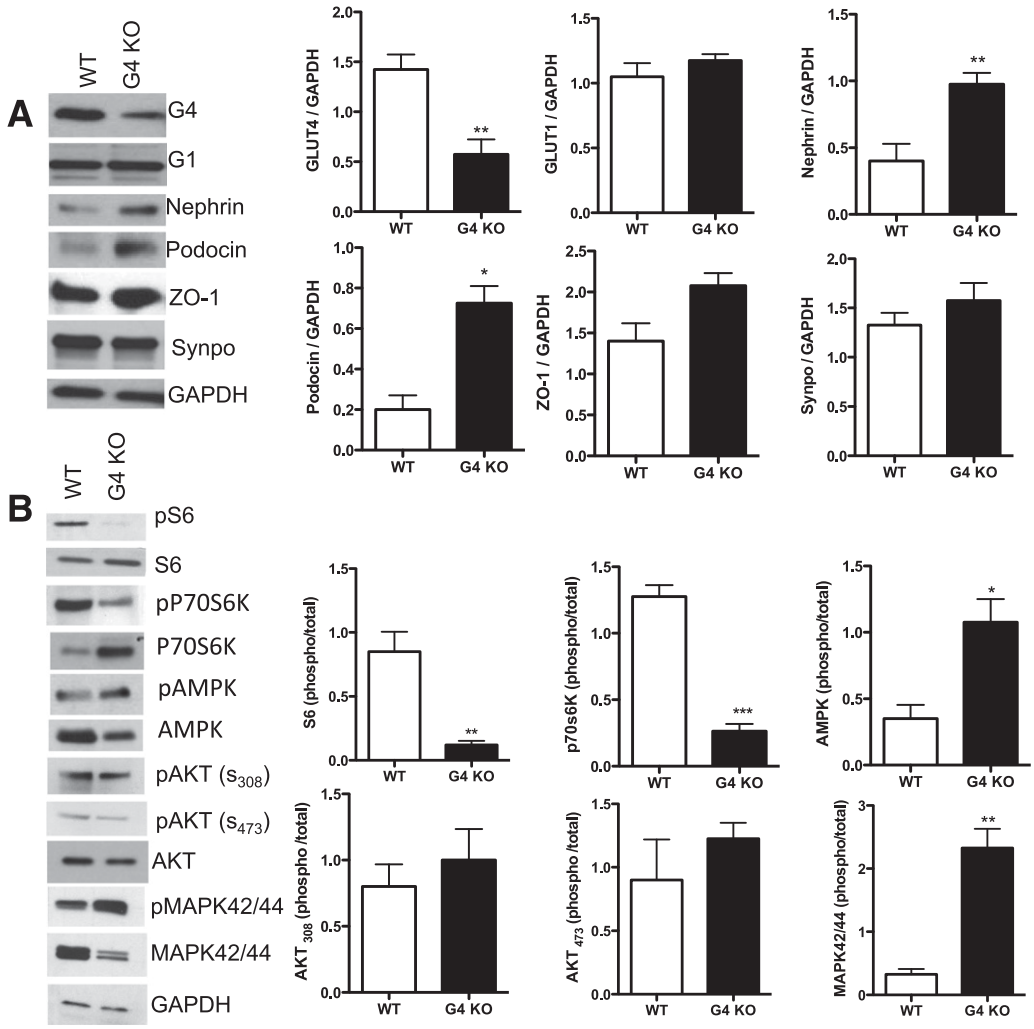

Figure 4—Glomeruli from G4 KO mice are characterized by increased synthesis of structural components and suppression of mTOR signaling. *A*: Representative Western blot analysis and relative bar graph quantification of proteins isolated from glomeruli microdissected and pooled from four WT and four G4 KO mice (representative of two separate experiments performed in duplicate) showing markedly reduced GLUT4 expression, unchanged GLUT1 expression, increased nephrin and podocin expression, and unchanged ZO-1 and synaptopodin expression. *B*: Western blot analysis of glomeruli from G4 KO mice demonstrating almost undetectable S6 and p70S6 phosphorylation with preserved AKT phosphorylation and increased AMPK and MAPK 42/44 phosphorylation when compared with WT. $^{*}P < 0.05$, $^{**}P < 0.01$, $^{***}P < 0.001$. p, phosphorylated; phospho, phosphorylation; Synpo, synaptopodin.

respectively; mean kidney weights were 0.3 g in each group; and mean blood glucose levels were 528, 570, and 542 mg/dL, respectively.

G4 KO Mice Are Protected From the Development of LPS-Induced Albuminuria

As LPS signaling requires activation of mTOR (33), we hypothesized that G4 KO mice would be resistant to albuminuria induced by LPS. As predicted, G4 KO mice were protected from the development of LPS-induced albuminuria (Fig. 8*A*). In fact, whereas LPS increased MyD88 in glomeruli from WT mice (Fig. 8*B*), such an increase was not observed in glomeruli from G4 KO mice. Deficient LPS signaling in G4 KO mice was also demonstrated by an inability of LPS to cause synaptopodin degradation (Fig. 8*B*). Nephrin subcellular distribution from a linear physiological pattern to a predominantly granular intracytoplasmic pattern was also observed in WT mice but not in G4 KO mice (Fig. 8*C*), and is consistent with the fact that mTORC1 activation results in nephrin mislocalization (19). Although LPS caused an increase in the phosphorylation of S6 in WT mice, this phenomenon was not observed in G4 KO mice (Fig. 8*D*).

Mice With a Podocyte-Specific Deletion of GLUT4 Are Susceptible to Adriamycin-Induced Nephropathy

As the suppression of the mTOR pathway augments the toxicity of adriamycin in cancer cells (37), we tested the hypothesis that G4 KO mice would become susceptible to adriamycin-induced nephropathy even on a background that is primarily C57BL6 and FVB, which are both known to be resistant to adriamycin-induced nephropathy (38).

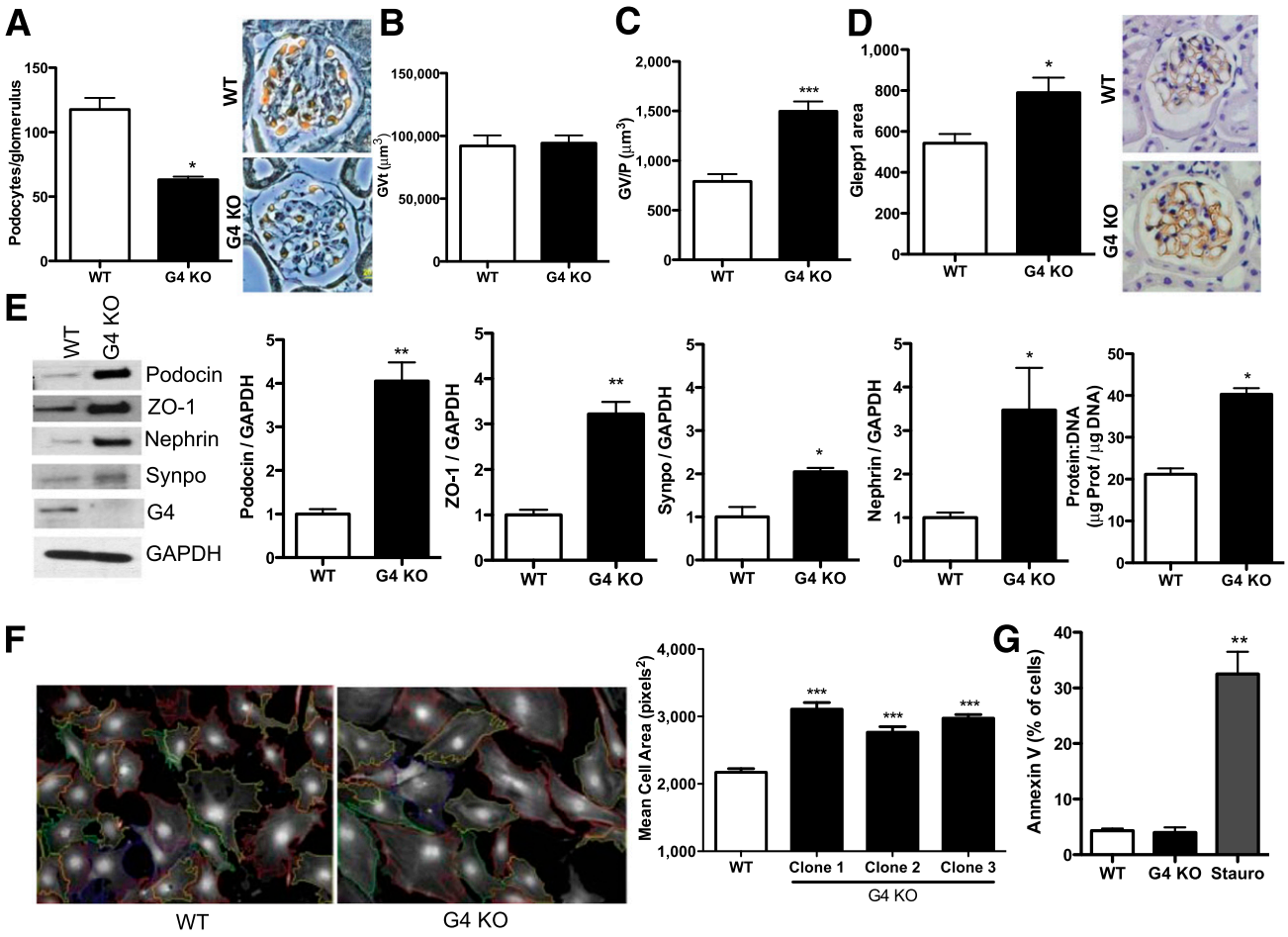

Figure 5—Podocyte-specific G4 KO mice have fewer and larger podocytes. *A*: Bar graph representation and representative image of the number of podocytes per glomerulus, which was significantly lower in G4 KO mice when compared with WT mice. G4 KO mice demonstrated no difference in glomerular volume (*B*), but increased GV/P (*C*), when compared with WT mice. *D*: Bar graph representation and representative image of G4 KO mice demonstrating a significantly higher GLEPP1-positive area when compared with WT mice. *E*: Representative Western blot analysis and relative bar graph analysis from primary podocyte cultures from three different G4 KO mice and WT mice. Undetectable GLUT4 confirmed effective recombination, and increased podocin, ZO-1, synaptopodin (Synpo), and nephrin expression was observed in G4 KO podocytes when compared with WT. Protein/DNA content was also increased in G4 KO podocytes when compared with WT mice. *F*: Quantitative analysis of cell size demonstrated increased cell size in each of three G4 KO cell lines when compared with the mean size of WT cell lines. *G*: Bar graph analysis of Annexin V staining (percentage of positive cells) in G4 KO podocytes when compared with WT or staurosporine-treated WT cells. $^{*}P < 0.05$, $^{**}P < 0.01$, $^{***}P < 0.001$.

While WT mice developed a mild mesangial expansion and albuminuria over time, G4 KO mice demonstrated a much higher degree of albuminuria at 3 weeks and increased mesangial expansion at 28 days after adriamycin administration (Fig. 9*A*–*C*). A significant reduction in podocyte number after adriamycin administration was observed in G4 KO mice but not in WT mice (Fig. 9*D*). Overall, these data suggested that GLUT4 deficiency may affect the development of proteinuria through an intrinsic inability to activate mTOR. To further test this hypothesis in vivo, we administered rapamycin to adriamycin-treated WT and G4 KO mice. Whereas rapamycin worsened albuminuria, mesangial expansion, and podocytopenia in WT mice (Fig. 9*E*–*H*), no changes were observed in G4 KO mice.

DISCUSSION

The ability of a cell to sense nutrients has emerged as a critical regulator of cellular homeostasis in several cell types including podocytes of the kidney glomerulus (17–19,39). Several key pathways are involved in nutrient sensing, such as mTOR, AMPK, and sirtuin (16). Among these pathways, mTOR signaling is suppressed when the deprivation of nutrients, such as glucose, occurs (40,41). Clinical and experimental data support a role for nutrient sensing in the pathogenesis of diabetes and its complications (16). However, key signaling elements of the nutrient-sensing pathway that may affect cell function even in the absence of diabetes or any metabolic disorders remain to be identified. It is possible that glucose uptake through facilitative GLUTs affects podocyte function

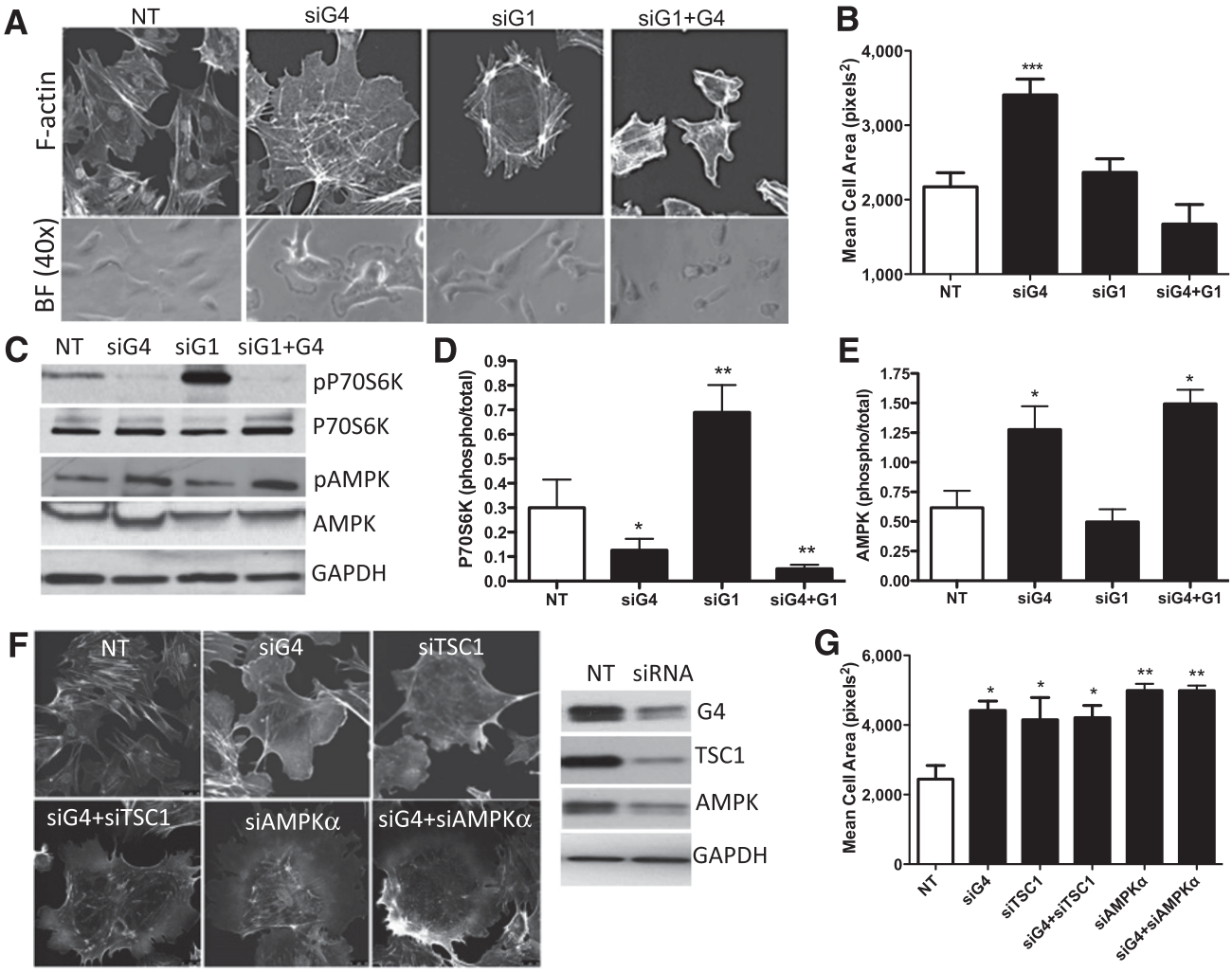

Figure 6—Podocyte hypertrophy is specific to GLUT4 deficiency, and is independent of mTOR and AMPK. *A*: siRNA for G4 (siG4) in mouse podocytes resulted in increased cell size as demonstrated in bright-field images (BF) and redistribution of F-actin as demonstrated by phalloidin staining (F-actin) 48 h after siRNA treatment. *B*: Quantitative analysis of cell size demonstrated increased cell size in siG4-treated cells when compared with siG1-treated cells and nontargeting siRNA-treated cells (NT). ***$P < 0.001$. *C*: Representative Western blot for phosphorylated and total P70S6K and AMPK in siG4, siG1, or siG4+G1 mouse podocytes. *D* and *E*: Bar graph analysis of P70S6K and AMPK (phosphorylated over total) in siG4, siG1, or siG4+G1 mouse podocytes. *$P < 0.05$, **$P < 0.01$. *F*: siRNA for TSC1 and for AMPKα in mouse podocytes was effective (representative Western blot), caused podocyte hypertrophy per se, but did not restore the hypertrophic phenotype of siG4 podocytes. *G*: Bar graph analysis for the quantitative evaluation of mean cell area in siRNA-treated mouse podocytes. *$P < 0.05$, **$P < 0.01$.

through the effect of podocytes on nutrient sensing, independently of extracellular glucose levels and of preserved insulin signaling. To address this question, we generated a podocyte-specific G4 KO mouse and investigated whether GLUT4 deficiency modulates podocyte function at baseline and in experimental models of proteinuria.

We focused our attention on GLUT4 because it is one of the major GLUTs expressed in podocytes (11,20), it has a predominant podocyte localization in the normal human kidney (Fig. 1*A*), and it is the most profoundly regulated GLUT after insulin stimulation (42). We found that whereas glomerular GLUT4 expression is upregulated in human and experimental nephropathy with normoalbuminuria and glomerular hypertrophy (Fig. 1*B* and *D*), it becomes downregulated once microalbuminuria develops (Fig. 1*C* and *E*). Upregulation of GLUT4 in early nephropathy occurs in podocytes and is accompanied by increased baseline glucose uptake, but a decrease insulin responsiveness (Fig. 2). Because insulin resistance appears to precede microalbuminuria (2,12), and because podocyte-specific IR deletion causes proteinuria (13), we expected that the deletion of the final downstream effector of insulin action (GLUT4) would result in a similar phenotype. To our surprise, no apparent renal phenotype was observed at baseline after podocyte-specific deletion of GLUT4 in mice (Fig. 3), suggesting that the phenotype of podocyte-specific IR-deficient mice is independent of GLUT4 expression. However,

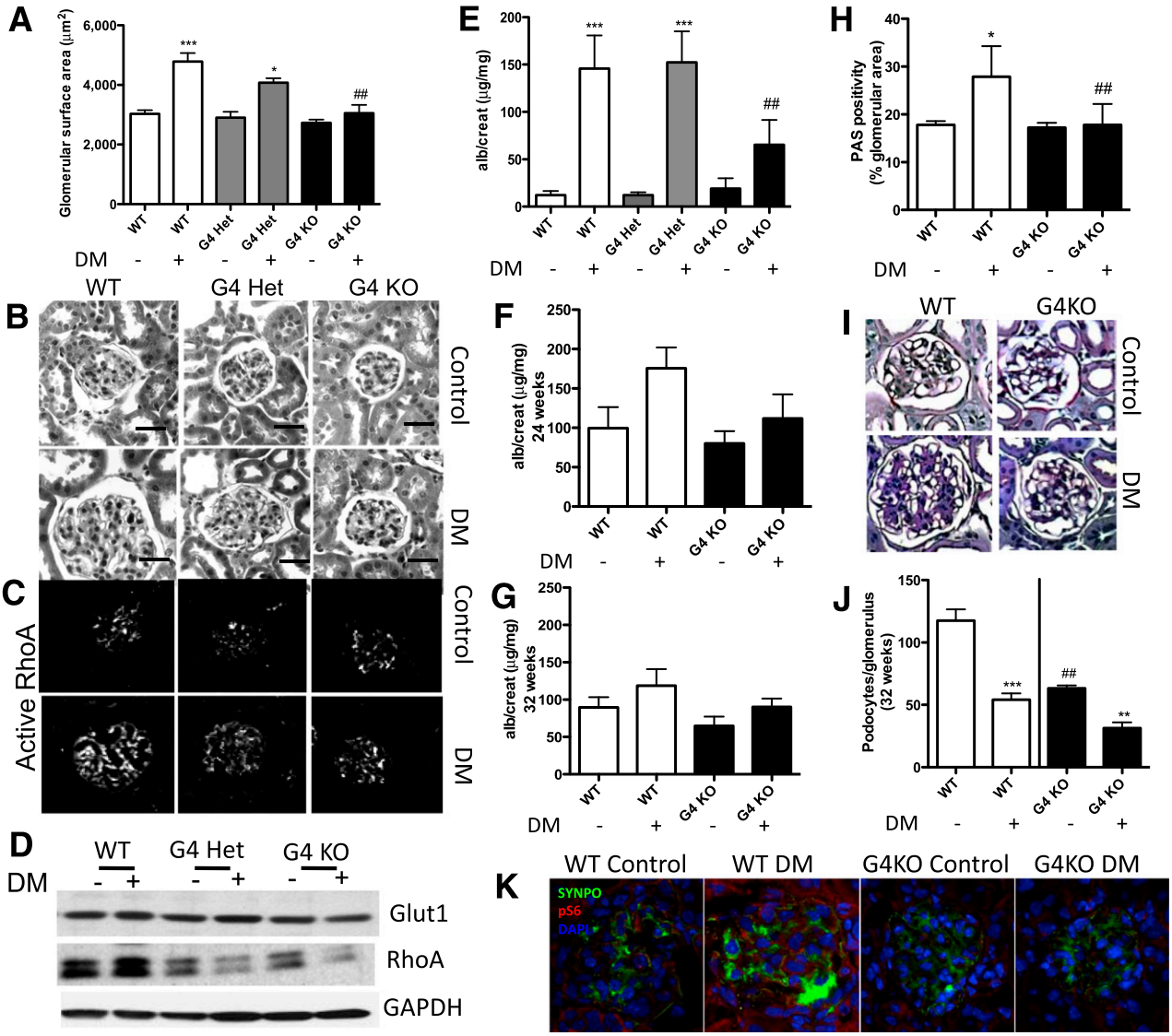

Figure 7—G4 KO mice are partially protected from the development of DN. *A*: Bar graph analysis of glomerular surface area of WT, G4 Het, and G4 KO mice with (DM+) or without (DM−) diabetes mellitus (DM). *B*: Representative PAS staining of glomeruli from WT, G4 Het, and G4 KO with diabetes or without diabetes (Control). *C*: Representative immunofluorescence staining showing increased active RhoA in glomeruli from WT diabetic mice; G4 KO glomeruli have less active RhoA at baseline as well as after the induction of diabetes. *D*: Western blot analysis of lysates obtained from pooled isolated glomeruli of WT, G4 Het, and G4 KO mice, demonstrating unchanged GLUT1 expression and increased RhoA expression in WT diabetic mice but not in G4 KO mice. *E*: Bar graph analysis of urinary albumin/creatinine (alb/creat) ratios in WT and G4 KO DM+ or DM− mice. G4 KO mice were partially protected from the development of albuminuria at 12 weeks, and this trend was partially preserved at 24 weeks (*F*) and at 32 weeks (*G*). Representative PAS images (*I*) and quantitative evaluation of PAS-positive glomerular area (*H*) in WT and G4 KO mice after 32 weeks with (DM) or without (Control) diabetes. *J*: Bar graph analysis of podocyte number in both WT and G4 KO DM+ or DM− mice. ***$P < 0.001$, **$P < 0.01$, *$P < 0.05$, when comparing diabetic mice to nondiabetic mice of the same genotype. ##$P < 0.01$ when comparing G4 KO diabetic mice to WT diabetic mice. *K*: Representative immunofluorescence confocal images for pS6 (red), synaptopodin (SYNPO; green), and DAPI (blue) in kidney sections from WT and G4 KO controls and DM mice.

podocyte-specific GLUT4 deficiency in vivo (Fig. 4) resulted in the activation of AMPK and the suppression of mTOR in isolated glomeruli. This is consistent with the observation that increased expression of GLUT4 in muscle fibers coincided with the activation of the mTOR pathway (43). Furthermore, there was a significant reduction in podocyte number (Fig. 5*A*), which has been shown to be a major mechanism driving glomerulosclerosis (44). Interestingly, this inborn reduction in podocyte number did not result in any structural glomerular pathology or any increase in albuminuria. In fact, as opposed to what was shown in the rat model of acquired podocytopenia, the decreased number of podocytes in our model was found to be associated with

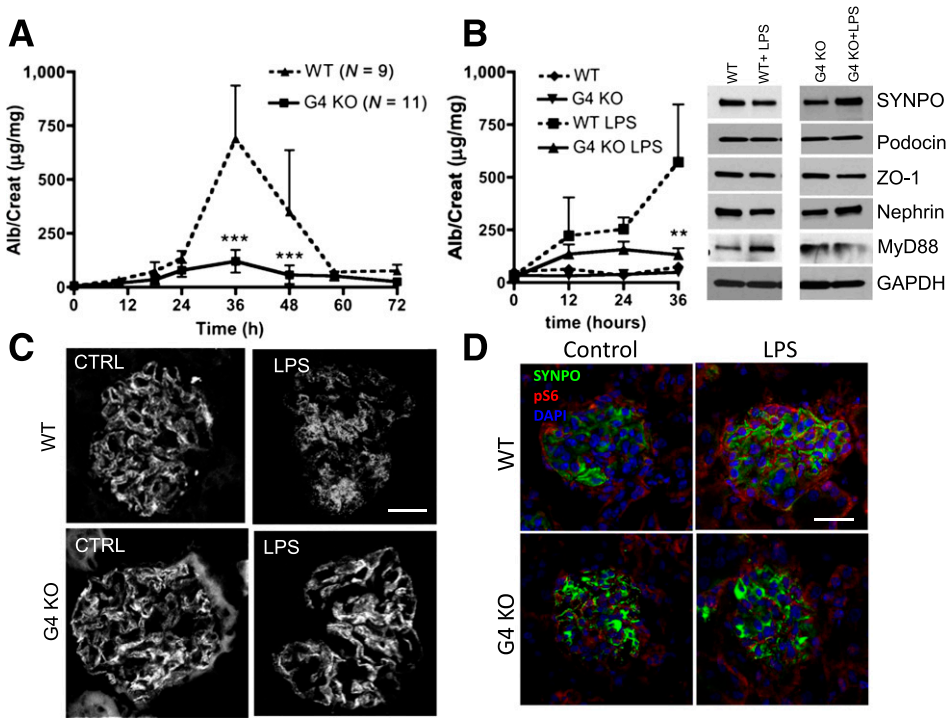

Figure 8—G4 KO mice are protected from LPS-induced proteinuria. *A*: Time course analysis of albumin/creatinine (Alb/Creat) ratios in morning urine collection in G4 KO (n = 11) and WT (n = 9) mice. *B*: The experiment was confirmed in a subsequent group of mice used to collect proteins from pooled microdissected glomeruli. Also shown in *B* is the Western blot analysis of pooled glomeruli collected 36 h after LPS injection at the time of maximal albuminuria from four mice per group, which demonstrated that, although systemic administration of LPS increases MyD88 in WT mice, LPS signaling is impaired in G4 KO mice, where the LPS-induced degradation of synaptopodin and nephrin is also prevented. *C*: Representative confocal images of nephrin in controls (CTRL) and LPS-treated mice. *D*: Representative immunofluorescence confocal images for pS6 (red), synaptopodin (SYNPO; green) and DAPI (blue) in controls (CTRL) and LPS-treated mice. Scale bar: 25 µm. $^{**}P < 0.01$, $^{***}P < 0.001$.

increased podocyte size in vivo (Fig. 5*D*) and in vitro (Figs. 5*F* and 6*A* and *B*), which occurred independently of mTOR, P70S6K, and AMPK.

Although primary mTORC1 activation has been clearly linked to podocyte hypertrophy (18,45), our data suggest that podocyte hypertrophy in G4 KO mice is mediated by an mTOR-independent mechanism. The possibility of mTOR-independent cellular hypertrophy is strongly supported by the evidence that mice with the cardiac overexpression of nonfunctional kinase-dead mTOR develop the same degree of cardiac hypertrophy compared with nontransgenic littermates (46). Moreover, the absence of albuminuria and glomerular pathology in podocyte-specific G4 KO mice demonstrates that inborn podocyte hypertrophy does not necessarily cause functional and pathologic changes in the glomerulus, as observed in forms of acquired maladaptive hypertrophy such as DN. Increased podocyte volume in G4 KO mice was associated with increased synthesis of structural components (Figs. 4*A* and 5*E*) and with the prevention of glomerular hypertrophy and glomerulosclerosis observed in WT mice in experimental models of diabetes (Fig. 7). This suggests that a primary form of adaptive podocyte hypertrophy, as observed in G4 KO mice, may provide protection from glomerular hypertrophy, whereas concomitant maladaptive podocyte and glomerular hypertrophy occurred in the aging rat (47) or in diabetic mice (18,19,45). Whether podocyte hypertrophy is the reason why G4 KO mice do not develop glomerular hypertrophy remains to be established. Although mTOR inhibition and AMPK activation could explain the lack of glomerular hypertrophy observed in G4 KO mice, increased slit-diaphragm proteins might contribute to diminishing albuminuria. It is possible that podocyte and glomerular volume in G4 KO mice are not related, and that G4 KO mice are protected from glomerular hypertrophy through similar mechanisms to those observed in calorie-restricted rats (32). Glomeruli from diabetic G4 KO mice also showed suppression of RhoA expression and activity (Fig. 7*D*), which is consistent with the finding that mTOR inhibition in cancer cells suppresses RhoA expression and activity (36). Although cardiac myocytes in heart-specific G4 KO mice develop hypertrophy (26), this could result from the marked compensatory increase in GLUT1 and glucose uptake found in the cardiac G4 KO model, which does not occur in the podocytes from podocyte-specific G4 KO mice and which has been shown to cause upregulation of mTOR in

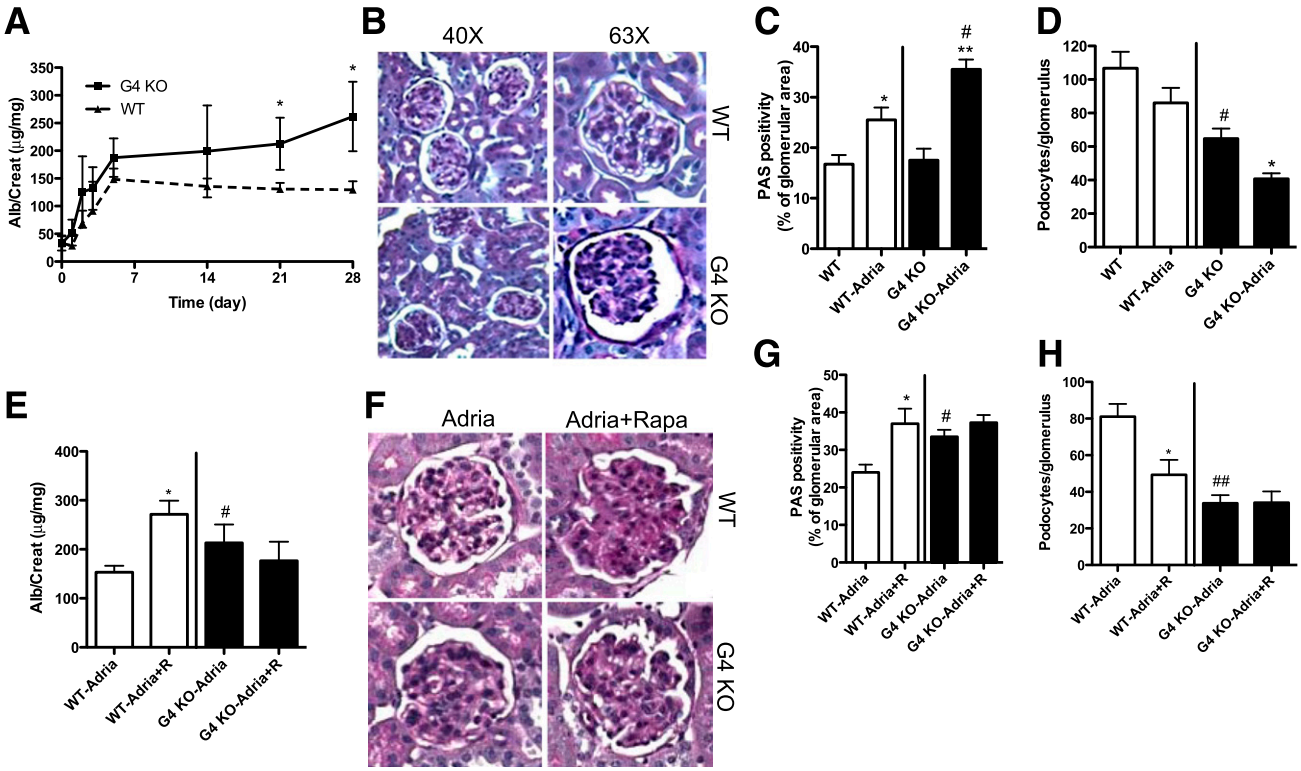

Figure 9—G4 KO mice develop worse adriamycin nephropathy than WT. *A*: Time course analysis of urinary albumin/creatinine (Alb/Creat) ratios in WT and G4 KO mice after a single dose of adriamycin at time 0. *B*: Representative low- and high-magnification images of PAS-stained tissue sections from adriamycin-treated WT and G4 KO mice. *C*: Bar graph analysis showing significant increase in mesangial expansion in G4 KO mice after adriamycin. Four mice per group were used. *D*: Bar graph representation of podocyte number showing significant reduction after adriamycin in G4 KO mice but not in WT mice. *E*: Time course analysis of urinary albumin/creatinine ratios in WT and G4 KO mice after a single dose of adriamycin followed by rapamycin injections three times per week over 5 weeks. Representative images of PAS-stained tissue sections (*F*), and bar graph analysis of mesangial expansion in adriamycin-treated and adriamycin-rapamycin–treated WT and G4 KO mice (*G*). *H*: Bar graph analysis showing significant decrease in the number of podocytes per glomerulus in WT after administration of adriamycin plus rapamycin, and no changes in GLUT4. $^{*}P < 0.05$, $^{**}P < 0.01$ when comparing treated mice to control mice of the same genotype. $\#P < 0.05$ and $\#\#P < 0.01$ when comparing GLUT4 KO mice to WT mice in the same treatment group. Adria, adriamycin; Rapa (or R), rapamycin.

mesangial cells (24). The apparent discrepancy related to the fact that G4 KO mice and podocyte-specific GLUT1-overexpressing mice are both protected from DN could be explained by the significant downregulation of GLUT4 expression in the latter model (25).

In order to investigate in vivo whether impaired mTOR signaling protects G4 KO mice from the development of DN, we used three independent experimental models of proteinuria that were previously linked to the mTOR signaling pathway. As mTOR inhibition prevents LPS signaling in neutrophils (33), we challenged G4 KO mice with LPS. As expected, we were able to show that LPS failed to signal and to cause proteinuria in G4 KO mice (Fig. 8*A* and *B*). Among other experimental models of proteinuria, adriamycin has been extensively used and usually leads to a phenotype that is very mild in mice with a background that is primarily FVB and C57Bl6, which is the background of the G4 KO mice (38). Importantly, however, adriamycin has been demonstrated to have an enhanced chemotherapeutic effect in the setting of mTOR inhibition (37). We therefore tested the hypothesis that G4 KO mice would develop a more severe renal phenotype than their WT littermates after exposure to adriamycin. Indeed, we were able to demonstrate that G4 KO mice were characterized by worsened albuminuria and mesangial expansion than WT mice after the administration of adriamycin. In order to establish a link between mTOR suppression and adriamycin toxicity in our model, we performed a third in vivo experiment and demonstrated that the addition of rapamycin to adriamycin worsened the renal phenotype of WT but not G4 KO mice (Fig. 9), consistent with the finding that rapamycin treatment aggravates the loss of glomerular filtration rate in patients with focal and segmental glomerulosclerosis (48). Our data suggest that the inability to activate mTOR in GLUT4-deficient hypertrophic podocytes may influence the development of proteinuria in experimental animals. However, restoration of mTOR or suppression of AMPK in GLUT4-deficient podocytes does not restore cell size. Whether GLUT4 deficiency influences mTOR-independent hypertrophic responses to natriuretic peptides, leucine, or

glutamate remains to be established. Furthermore, our data suggest a functional dissociation between IR and GLUT4 signaling. In fact, as insulin sensitizers improve albuminuria in clinical and experimental studies (49–51), one may expect that GLUT4 deficiency would result in a disease phenotype attributable to the alteration of the physiological regulation of glucose uptake in response to insulin, as suggested based on prior studies from us and others (14). However, our findings obtained with the in vivo models do not support this hypothesis and add further complexity to the role of insulin signaling in podocyte function. Our in vivo observations are also consistent with the fact that insulin sensitizers of this class of thiazolidinediones prevent mTOR-dependent signaling (52) while facilitating insulin signaling in several cells, including the podocyte (53). Additional studies are needed to investigate whether the function of GLUT4 in podocyte is independent of insulin signaling. In this respect, it would be interesting to determine whether podocyte-specific deletion of GLUT4 is sufficient to restore the glomerular phenotype of mice with a podocyte-specific deletion of the IR. The evidence that GLUT4 binds aldolase, which is known to interact with actin, suggests that GLUT4 may directly regulate actin remodeling (54). Finally, our data suggest that GLUT4 may regulate podocyte function and that strategies that decrease GLUT4 expression and/or function may be beneficial in proteinuric kidney diseases.

Acknowledgments. The authors thank MaryLee Schin (University of Michigan) for technical assistance and assistance with immunostaining and morphometry.

Funding. E.D.A. was supported by National Institutes of Health grant U01HL087947. A.F. and S.M.-G. were supported by National Institutes of Health grant DK-090316, the Forest County Potawatomi Community Foundation, the Max and Yetta Karasik Family Foundation, the Diabetes Research Institute Foundation (diabetesresearch.org), the Diabetic Complications Consortium (DiaComp), and the Peggy and Harold Katz Family Foundation. S.M.-G. was also supported by the Stanley J. Glaser Foundation Research Award. A.F. was also supported by grant 1UL1TR000460, University of Miami Clinical and Translational Science Institute, from the National Center for Advancing Translational Sciences, and the National Institute on Minority Health and Health Disparities.

Duality of Interest. No potential conflicts of interest relevant to this article were reported.

Author Contributions. J.G. performed some of the in vivo experiments and the isolation of primary podocytes. A.N.J. performed some of the in vitro experiments and the siRNA experiments. S.M.-G. designed the in vivo experiments and assisted in results interpretation. D.M. performed immunofluorescence studies. C.M. maintained the mice colony. A.M., T.-H.Y., R.V., and C.P. performed Western blot analysis and urine analysis. A.D.-S. studied protein content and glucose uptake. J.Sz. collected and analyzed human samples, and performed all the quantitative histological readouts. R.D.M. assisted with killing of the mice. K.J. processed tissue samples. B.K. and E.D.A. provided the mice and assisted in results interpretation. B.H. contributed to the analysis of podocyte size. T.B.H. and G.W.B. helped with the interpretation of results and manuscript preparation. J.Sa. contributed to the analysis of histological variables from tissue sections. F.C.B. and A.F. wrote the manuscript. A.F. is the guarantor of this work and, as such, had full access to all the data in the study and takes responsibility for the integrity of the data and the accuracy of the data analysis.

Prior Presentation. Parts of this study were presented in abstract form at the European Diabetic Neuropathy Study Group, Stockholm, Sweden, 7–9 June 2012; the American Society of Nephrology Kidney Week 2011, Philadelphia, PA, 10–12 November 2011; and the 9th International Podocyte Conference, Miami, FL, 21–25 November 2012.

References

1. Mogensen CE, Christensen NJ, Gundersen HJ. The acute effect of insulin on heart rate, blood pressure, plasma noradrenaline and urinary albumin excretion. The role of changes in blood glucose. Diabetologia 1980;18:453–457
2. Ekstrand AV, Groop PH, Grönhagen-Riska C. Insulin resistance precedes microalbuminuria in patients with insulin-dependent diabetes mellitus. Nephrol Dial Transplant 1998;13:3079–3083
3. Yip J, Mattock MB, Morocutti A, Sethi M, Trevisan R, Viberti G. Insulin resistance in insulin-dependent diabetic patients with microalbuminuria. Lancet 1993;342:883–887
4. Groop L, Ekstrand A, Forsblom C, et al. Insulin resistance, hypertension and microalbuminuria in patients with type 2 (non-insulin-dependent) diabetes mellitus. Diabetologia 1993;36:642–647
5. Parvanova AI, Trevisan R, Iliev IP, et al. Insulin resistance and microalbuminuria: a cross-sectional, case-control study of 158 patients with type 2 diabetes and different degrees of urinary albumin excretion. Diabetes 2006;55:1456–1462
6. Forsblom CM, Eriksson JG, Ekstrand AV, Teppo AM, Taskinen MR, Groop LC. Insulin resistance and abnormal albumin excretion in non-diabetic first-degree relatives of patients with NIDDM. Diabetologia 1995;38:363–369
7. Yip J, Mattock M, Sethi M, Morocutti A, Viberti G. Insulin resistance in family members of insulin-dependent diabetic patients with microalbuminuria. Lancet 1993;341:369–370
8. Mykkänen L, Zaccaro DJ, Wagenknecht LE, Robbins DC, Gabriel M, Haffner SM. Microalbuminuria is associated with insulin resistance in nondiabetic subjects: the insulin resistance atherosclerosis study. Diabetes 1998;47:793–800
9. Musso C, Javor E, Cochran E, Balow JE, Gorden P. Spectrum of renal diseases associated with extreme forms of insulin resistance. Clin J Am Soc Nephrol 2006;1:616–622
10. Faul C, Asanuma K, Yanagida-Asanuma E, Kim K, Mundel P. Actin up: regulation of podocyte structure and function by components of the actin cytoskeleton. Trends Cell Biol 2007;17:428–437
11. Coward RJ, Welsh GI, Yang J, et al. The human glomerular podocyte is a novel target for insulin action. Diabetes 2005;54:3095–3102
12. Tejada T, Catanuto P, Ijaz A, et al. Failure to phosphorylate AKT in podocytes from mice with early diabetic nephropathy promotes cell death. Kidney Int 2008;73:1385–1393
13. Welsh GI, Hale LJ, Eremina V, et al. Insulin signaling to the glomerular podocyte is critical for normal kidney function. Cell Metab 2010;12:329–340
14. Fornoni A. Proteinuria, the podocyte, and insulin resistance. N Engl J Med 2010;363:2068–2069
15. Pessin JE, Saltiel AR. Signaling pathways in insulin action: molecular targets of insulin resistance. J Clin Invest 2000;106:165–169
16. Kume S, Thomas MC, Koya D. Nutrient sensing, autophagy, and diabetic nephropathy. Diabetes 2012;61:23–29

17. Eid AA, Ford BM, Block K, et al. AMP-activated protein kinase (AMPK) negatively regulates Nox4-dependent activation of p53 and epithelial cell apoptosis in diabetes. J Biol Chem 2010;285:37503–37512
18. Gödel M, Hartleben B, Herbach N, et al. Role of mTOR in podocyte function and diabetic nephropathy in humans and mice. J Clin Invest 2011;121: 2197–2209
19. Inoki K, Mori H, Wang J, et al. mTORC1 activation in podocytes is a critical step in the development of diabetic nephropathy in mice. J Clin Invest 2011;121:2181–2196
20. Moutzouris DA, Kitsiou PV, Talamagas AA, Drossopoulou GI, Kassimatis TI, Katsilambros NK. Chronic exposure of human glomerular epithelial cells to high glucose concentration results in modulation of high-affinity glucose transporters expression. Ren Fail 2007;29:353–358
21. Schiffer M, Susztak K, Ranalletta M, Raff AC, Böttinger EP, Charron MJ. Localization of the GLUT8 glucose transporter in murine kidney and regulation in vivo in nondiabetic and diabetic conditions. Am J Physiol Renal Physiol 2005;289:F186–F193
22. Lewko B, Bryl E, Witkowski JM, et al. Characterization of glucose uptake by cultured rat podocytes. Kidney Blood Press Res 2005;28:1–7
23. Wang Y, Heilig K, Saunders T, et al. Transgenic overexpression of GLUT1 in mouse glomeruli produces renal disease resembling diabetic glomerulosclerosis. Am J Physiol Renal Physiol 2010;299:F99–F111
24. Buller CL, Heilig CW, Brosius FC 3rd. GLUT1 enhances mTOR activity independently of TSC2 and AMPK. Am J Physiol Renal Physiol 2011;301:F588–F596
25. Zhang H, Schin M, Saha J, et al. Podocyte-specific overexpression of GLUT1 surprisingly reduces mesangial matrix expansion in diabetic nephropathy in mice. Am J Physiol Renal Physiol 2010;299: F91–F98
26. Abel ED, Kaulbach HC, Tian R, et al. Cardiac hypertrophy with preserved contractile function after selective deletion of GLUT4 from the heart. J Clin Invest 1999;104:1703–1714
27. Moeller MJ, Sanden SK, Soofi A, Wiggins RC, Holzman LB. Podocyte-specific expression of cre recombinase in transgenic mice. Genesis 2003;35:39–42
28. Atkins KB, Prezkop A, Park JL, et al. Preserved expression of GLUT4 prevents enhanced agonist-induced vascular reactivity and MYPT1 phosphorylation in hypertensive mouse aorta. Am J Physiol Heart Circ Physiol 2007;293:H402–H408
29. Faul C, Donnelly M, Merscher-Gomez S, et al. The actin cytoskeleton of kidney podocytes is a direct target of the antiproteinuric effect of cyclosporine A. Nat Med 2008;14:931–938
30. Zhang H, Saha J, Byun J, et al. Rosiglitazone reduces renal and plasma markers of oxidative injury and reverses urinary metabolite abnormalities in the amelioration of diabetic nephropathy. Am J Physiol Renal Physiol 2008;295:F1071–F1081
31. Sanden SK, Wiggins JE, Goyal M, Riggs LK, Wiggins RC. Evaluation of a thick and thin section method for estimation of podocyte number, glomerular volume, and glomerular volume per podocyte in rat kidney with Wilms' tumor-1 protein used as a podocyte nuclear marker. J Am Soc Nephrol 2003;14:2484–2493
32. Fukuda A, Chowdhury MA, Venkatareddy MP, et al. Growth-dependent podocyte failure causes glomerulosclerosis. J Am Soc Nephrol 2012;23:1351–1363
33. Lorne E, Zhao X, Zmijewski JW, et al. Participation of mammalian target of rapamycin complex 1 in Toll-like receptor 2- and 4-induced neutrophil activation and acute lung injury. Am J Respir Cell Mol Biol 2009;41:237–245
34. Kolavennu V, Zeng L, Peng H, Wang Y, Danesh FR. Targeting of RhoA/ROCK signaling ameliorates progression of diabetic nephropathy independent of glucose control. Diabetes 2008;57:714–723
35. Peng F, Wu D, Gao B, et al. RhoA/Rho-kinase contribute to the pathogenesis of diabetic renal disease. Diabetes 2008;57:1683–1692
36. Liu L, Luo Y, Chen L, et al. Rapamycin inhibits cytoskeleton reorganization and cell motility by suppressing RhoA expression and activity. J Biol Chem 2010;285:38362–38373
37. Piguet AC, Semela D, Keogh A, et al. Inhibition of mTOR in combination with doxorubicin in an experimental model of hepatocellular carcinoma. J Hepatol 2008;49:78–87
38. Lee VW, Harris DC. Adriamycin nephropathy: a model of focal segmental glomerulosclerosis. Nephrology (Carlton) 2011;16:30–38
39. Hallows KR, Mount PF, Pastor-Soler NM, Power DA. Role of the energy sensor AMP-activated protein kinase in renal physiology and disease. Am J Physiol Renal Physiol 2010;298:F1067–F1077
40. Wellen KE, Thompson CB. Cellular metabolic stress: considering how cells respond to nutrient excess. Mol Cell 2010;40:323–332
41. Zoncu R, Efeyan A, Sabatini DM. mTOR: from growth signal integration to cancer, diabetes and ageing. Nat Rev Mol Cell Biol 2011;12:21–35
42. Lennon R, Pons D, Sabin MA, et al. Saturated fatty acids induce insulin resistance in human podocytes: implications for diabetic nephropathy. Nephrol Dial Transplant 2009;24:3288–3296
43. Stuart CA, Howell ME, Baker JD, et al. Cycle training increased GLUT4 and activation of mammalian target of rapamycin in fast twitch muscle fibers. Med Sci Sports Exerc 2010;42:96–106
44. Wharram BL, Goyal M, Wiggins JE, et al. Podocyte depletion causes glomerulosclerosis: diphtheria toxin-induced podocyte depletion in rats expressing human diphtheria toxin receptor transgene. J Am Soc Nephrol 2005;16:2941–2952
45. Kim DK, Nam BY, Li JJ, et al. Translationally controlled tumour protein is associated with podocyte hypertrophy in a mouse model of type 1 diabetes. Diabetologia 2012;55:1205–1217
46. Shen WH, Chen Z, Shi S, et al. Cardiac restricted overexpression of kinase-dead mammalian target of rapamycin (mTOR) mutant impairs the mTOR-mediated signaling and cardiac function. J Biol Chem 2008;283:13842–13849
47. Wiggins JE, Goyal M, Sanden SK, et al. Podocyte hypertrophy, "adaptation," and "decompensation" associated with glomerular enlargement and glomerulosclerosis in the aging rat: prevention by calorie restriction. J Am Soc Nephrol 2005;16:2953–2966
48. Cho ME, Hurley JK, Kopp JB. Sirolimus therapy of focal segmental glomerulosclerosis is associated with nephrotoxicity. Am J Kidney Dis 2007;49:310–317
49. Miyazaki Y, Cersosimo E, Triplitt C, DeFronzo RA. Rosiglitazone decreases albuminuria in type 2 diabetic patients. Kidney Int 2007;72:1367–1373
50. Ohtomo S, Izuhara Y, Takizawa S, et al. Thiazolidinediones provide better renoprotection than insulin in an obese, hypertensive type II diabetic rat model. Kidney Int 2007;72:1512–1519
51. Schernthaner G, Matthews DR, Charbonnel B, Hanefeld M, Brunetti P; Quartet [corrected] Study Group. Efficacy and safety of pioglitazone versus metformin in patients with type 2 diabetes mellitus: a double-blind, randomized trial. J Clin Endocrinol Metab 2004;89:6068–6076
52. Kim JS, Kim IK, Lee SY, et al. The anti-proliferative effect of rosiglitazone on angiotensin II-induced vascular smooth muscle cell proliferation is mediated by the mTOR pathway. Cell Biol Int 2012;36:305–310
53. Lennon R, Welsh GI, Singh A, et al. Rosiglitazone enhances glucose uptake in glomerular podocytes using the glucose transporter GLUT1. Diabetologia 2009;52:1944–1952
54. Kao AW, Noda Y, Johnson JH, Pessin JE, Saltiel AR. Aldolase mediates the association of F-actin with the insulin-responsive glucose transporter GLUT4. J Biol Chem 1999;274:17742–17747